Published in final edited form as:
Radiat Res. 2001 February ; 155(2): 335–344.

Free Radical-Initiated and Gap Junction-Mediated Bystander Effect due to Nonuniform Distribution of Incorporated Radioactivity in a Three-Dimensional Tissue Culture Model

Anupam Bishayee[a], **Helene Z. Hill**[a], **Dana Stein**[b], **Dandamudi V. Rao**[a,1], and **Roger W. Howell**[a,2]

[a]Division of Radiation Research, Department of Radiology, University of Medicine and Dentistry of New Jersey-New Jersey Medical School, Newark, New Jersey 07103

[b]Department of Pediatrics, University of Medicine and Dentistry of New Jersey-New Jersey Medical School, Newark, New Jersey 07103

Abstract

To investigate the biological effects of nonuniform distribution of radioactivity in mammalian cells, we have developed a novel three-dimensional tissue culture model. Chinese hamster V79 cells were labeled with tritiated thymidine and mixed with unlabeled cells, and multicellular clusters (~1.6 mm in diameter) were formed by gentle centrifugation. The short-range β particles emitted by ^{3}H impart only self-irradiation of labeled cells without significant cross-irradiation of unlabeled bystander cells. The clusters were assembled in the absence or presence of 10% dimethyl sulfoxide (DMSO) and/or 100 μ*M* lindane. DMSO is a hydroxyl radical scavenger, whereas lindane is an inhibitor of gap junctional intercellular communication. The clusters were maintained at 10.5°C for 72 h to allow ^{3}H decays to accumulate and then dismantled, and the cells were plated for colony formation. When 100% of the cells were labeled, the surviving fraction was exponentially dependent on the mean level of radioactivity per labeled cell. A two-component exponential response was observed when either 50 or 10% of the cells were labeled. Though both DMSO and lindane significantly protected the unlabeled or bystander cells when 50 or 10% of the cells were labeled, the effect of lindane was greater than that of DMSO. In both cases, the combined treatment (DMSO + lindane) elicited maximum protection of the bystander cells. These results suggest that the bystander effects caused by nonuniform distributions of radioactivity are affected by the fraction of cells that are labeled. Furthermore, at least a part of these bystander effects are initiated by free radicals and are likely to be mediated by gap junctional intercellular communication.

INTRODUCTION

There is substantial interest in the role of bystander effects in the biological response of mammalian cells to ionizing radiation. It has long been believed that the principal genetic effects of ionizing radiation in mammalian cells are the direct result of DNA damage in irradiated cells that has not been repaired adequately. Therefore, when cells are exposed to external beams of radiation, only those cells that receive “hits” from the emitted radiations would be damaged. No effects would be observed in cells that are not “hit.” These cells are

[2]Author to whom correspondence should be addressed at Division of Radiation Research, Department of Radiology, MSB F-451, University of Medicine and Dentistry of New Jersey-New Jersey Medical School, 185 South Orange Avenue, Newark, NJ 07103.
[1]Present address: 2637 S. Saks Pt., Inverness, FL 34450.

referred to as bystanders. Studies from a number of laboratories suggest that these bystander cells do indeed incur damage as a consequence of being in the neighborhood of irradiated cells (1). Nagasawa and Little (2) first showed that Chinese hamster ovary (CHO) cells exposed to very low fluences of α particles exhibited a much higher incidence of cells with sister chromatid exchanges (SCEs) than expected based on the number of cells that were traversed by α particles. These authors found similar results when induction of *HPRT* mutations was used as the end point, thereby confirming that genetic damage does occur in bystander cells that are not irradiated (3). Deshpande *et al.* (4) reported increases of more than eightfold in the percentage of primary human fibroblast cells expressing an increased level of SCE over the actual number of nuclei traversed by an α particle. Hickman *et al.* (5) documented that α particles induced accumulation of the Tp53 tumor suppressor protein in rat lung epithelial cells in a higher percentage of cells than expected based on the number that would have received a direct nuclear traversal. Azzam *et al.* (6) made similar observations with altered expression of TP53, CDKN1A (also known as $p21^{Waf1}$), CDC2 (also known as $p34^{cdc2}$), cyclin B1 and RAD51 in human diploid fibroblast cells. Prise *et al.* (7) reported a higher frequency of apoptotic and micronucleated human fibroblast cells in cultures irradiated with a charged $^{3}He^{2+}$ particle microbeam. Mothersill and Seymour (8) demonstrated that addition of medium from epithelial cells irradiated with γ rays led to increased cell death and apoptosis of unirradiated cells.

Although consistent support for the existence of bystander effects is available in the literature, studies that probe the mechanisms that lead to damage in bystander cells are limited. Bystander effects have been attributed to the production of extracellular factors that lead to the generation of reactive oxygen species (ROS) (9–11). More recently, Iyer and Lehnert (12) have postulated that transforming growth factor β1 is the mediator of α-particle-induced bystander responses. Gap junctional intercellular communication (GJIC) has also been implicated as one of the mechanisms (6, 13). It has also been suggested that other mechanisms such as extranuclear-originating signal pathways, secreted diffusible factors, and apoptosis-inducing factors may be involved in the responses of bystander cells (14, 15). These findings suggest that different mechanisms may be operational for bystander effects depending on the cell type, the type of radiation, and other experimental conditions, including the end points studied.

The issue of bystander effects is relevant to the biological effects of nonuniform distribution of radioactivity; however, there is a paucity of data. This is of major importance to risk estimation in diagnostic nuclear medicine and radiation protection (e.g. inhalation of radon/radon progeny) as well as clinical outcome in therapeutic nuclear medicine. One of the major obstacles to predicting the biological response of tissues with nonuniform distribution of radioactivity is the absence of suitable experimental models that allow precise control of the degree of nonuniformity. To overcome this problem, we have recently developed a novel three-dimensional tissue culture model (13). Using this model, we have shown evidence of pronounced bystander effects in the form of decreased cell survival when ^{3}H is localized in the DNA of Chinese hamster lung fibroblast (V79) cells and is distributed nonuniformly in multicellular clusters (13). In the present communication, the same multicellular cluster model is used to investigate the impact of different magnitudes of nonuniform distribution of radioactivity on bystander effects. The underlying mechanisms of bystander effects that arise from nonuniform distribution of radioactivity are also studied.

MATERIALS AND METHODS

Radiochemical and its Quantification

Tritiated thymidine ([^{3}H]dThd) was obtained from NEN Life Science Products (Boston, MA) as a sterile aqueous solution at a concentration of 37 MBq/ml with a specific activity of

3000 GBq/mmol. The activity of ^{3}H was measured with a Beckman LS3800 automatic liquid scintillation counter (Fullerton, CA). The detection efficiency for the β particles emitted by ^{3}H was 0.65.

Cell Culture

V79 cells, kindly provided by Dr. A. I. Kassis (Harvard Medical School, Boston, MA), were used in the present study, with clonogenic survival serving as the biological end point. V79 cells are known to exhibit some degree of GJIC (16–18). The different minimum essential media (MEMA, MEMB and wash MEMA) and culturing conditions have been described in detail previously (13). The plating efficiency was about 64%.

Assembly of Multicellular Clusters

The protocols were as described earlier (13). Briefly, V79 cells were conditioned in 1 ml MEMB in 17 × 100-mm Falcon polypropylene culture tubes placed on a rocker-roller for 3–4 h in an incubator at 37°C, 5% CO_2, 95% air (2 or 4 × 10^6 cells/ml). Thereafter, 1 ml MEM containing various activities of [^{3}H]dThd was added and the tubes were returned to the rocker-roller. After 12 h, the cells were washed three times with wash MEMA, resuspended in 2 ml of MEMA, and passed several times through a 21 gauge needle. Additional tubes containing cells not labeled with ^{3}H were processed identically. The radiolabeled cells were then mixed with unlabeled cells to get 100, 50 or 10% radiolabeled cells, pelleted and transferred directly to a sterile 400-μl polypropylene microcentrifuge tube (Helena Plastics, San Rafael, CA). The tubes were centrifuged at 1000 rpm for 5 min at 4°C to form clusters with diameter ~1.6 mm (4 × 10^6 cells).

Treatment with DMSO and/or Lindane

To study the mechanisms underlying bystander effects, the multicellular clusters were assembled in the presence of the free radical scavenger DMSO and/or an inhibitor of GJIC, lindane (Sigma Chemical Co., St. Louis, MO). To achieve radioprotection, a DMSO concentration of 10% (1.28 *M*) was required as per our previous studies (19). Lindane was dissolved in DMSO (5 mg/ml) and subsequently diluted with MEMA to a final concentration of 100 μ*M* lindane–0.58% DMSO. These concentrations of lindane and DMSO were not cytotoxic (13).

Cell Survival

The microcentrifuge tubes containing the clusters were maintained at 10.5°C for 72 h to allow decay of ^{3}H in the absence of cell division. Under these conditions, V79 cells can withstand prolonged exposure to 10% DMSO and 100 μ*M* lindane without significant loss of plating efficiency (13, 19). The supernatant was then carefully removed and the tubes were vortexed to disperse the cell clusters. The cells were washed three times with 10 ml of wash MEMA, resuspended in 2 ml of wash MEMA, passed several times through a 21-gauge needle (resulting in a single cell suspension with a doublet frequency of only 2.4%), serially diluted, seeded in triplicate into 60 × 15-mm Falcon tissue culture dishes, and incubated at 37°C with 95% air and 5% CO_2. Aliquots were taken from each tube before serial dilution as above, and the mean radioactivity per cell was determined. After 7 days, the surviving fraction compared to control cells was determined.

Kinetics of Radioactivity in Cells

To ascertain the absorbed dose received by the cells, the kinetics of uptake and clearance of the radioactivity from the cells was followed. Multicellular clusters were prepared with 100% of the cells labeled as described above. At various times after the clusters were placed at 10.5°C, a cluster was dismantled and the level of radioactivity per cell was determined.

Additionally, cells from clusters that had been maintained at 10.5°C for 72 h were washed with wash MEMA, and 1×10^6, 5×10^5, 2.5×10^5 and 2.5×10^5 cells were finally plated in duplicate into 75-cm^2 culture flasks. On each of the following 4 days, duplicate flasks with the same number of cells plated (in descending order) were removed from the incubator and the activity per cell was determined.

Monitoring of Radioactivity in Labeled and Unlabeled Cells

Studies were carried out to trace radioactivity in the labeled and unlabeled cells. The radiolabeled cells were dyed with 0.05 μ*M* carboxyfluorescein diacetate succinimidyl ester (CFDA SE) in phosphate-buffered saline (PBS) at 37°C for 15 min using a Vybranty™ cell tracer kit (Molecular Probes, Eugene, OR). CFDA SE passively diffuses into cells, where its acetate groups are cleaved by intercellular esterases to yield the highly fluorescent carboxyfluorescein succinimidyl ester that reacts with intracellular amines forming well-retained fluorescent conjugates. The radiolabeled and dyed cells (2×10^6) were mixed with an equal number of unlabeled, undyed cells. The pooled cells were used to form clusters containing a total of 4×10^6 cells (50% of the cells were radiolabeled and dyed) and the clusters were maintained at 10.5°C. After 72 h, the cells from two clusters were pooled, washed with PBS, resuspended in 5 μ*M* EDTA in PBS to a concentration of 10^7 cells/ml, and passed through a 21-gauge needle five times to produce a single cell suspension. The cells were subjected to fluorescence-activated cell sorting (FACS) using a FACSCalibur flow cytometer (Becton Dickinson, San Francisco, CA). An air-cooled 488-nm argon-ion laser was used to excite the dye. The excitation and emission peaks of the fluorescent dye are 492 and 517 nm, respectively. Fluorescence in the FL-1 channel was collected along with forward-angle and 90° light scatter. The cells were sorted for dye-negative cells. A gate was applied around the cell population to evaluate cellular events. Single-parameter histograms based on 10,000 events were analyzed using CellQUEST software (Becton Dickinson). After sorting, the dye-negative cells (unlabeled and undyed) were collected, pooled, washed and finally resuspended in 2 ml of 5 μ*M* EDTA in PBS. Aliquots were used to determine the mean activity per cell. An additional 0.5 ml of the suspension was subjected to FACS for the second time to check the purity of sorted cells (i.e. absence of dye-positive cells).

Assessment of GJIC by Flow Cytometry

The presence of functional GJIC between V79 cells in multicellular clusters maintained at 10.5°C in the absence and presence of lindane was monitored by flow cytometry. The method of Goldberg *et al.* (20) was used with modifications. Cells (4 or 2×10^6) were loaded with calcein AM (Molecular Probes). This fluorescent dye becomes membrane impermeant when it enters the cell. However, it can traverse functional gap junctions (21). The loading was achieved by incubating cells for 25 min at 37°C in the presence of 2 ml of 20 μ*M* dye in PBS. The cells were then washed with PBS, resuspended in prewarmed MEMA, incubated at 37°C for 30 min, and centrifuged, and the supernatant was decanted. Undyed cells were treated similarly. These cells were used to form multicellular clusters containing 100 or 50% dyed cells. The clusters with 50% dyed cells were prepared in the presence or absence of 100 μ*M* lindane. The clusters were then maintained at 10.5°C for 72 h. The cells from clusters were washed with PBS and resuspended in 1 ml of 5 μ*M* EDTA in PBS. In the lindane-treated cells, all steps after the dyeing procedure, including washes and resuspensions, were carried out in the presence of lindane. GJIC was interpreted as the ability of the dye to pass from pre-dyed cells to undyed cells. This was determined by measuring the fluorescence of cells with the FACSCaliber flow cytometer with a 530-nm band pass filter using the technique of Tomasetto *et al.* (22). Fluorescent signals were processed over a four-decade logarithmic range. The clusters containing 100% dyed and undyed cells served as positive and negative controls. A no-dye-transfer control for the 50%

dyed cell clusters was prepared by mixing equal volumes of the final suspensions of the 100% dyed and undyed cells, and the resulting mixture was immediately analyzed with the flow cytometer.

RESULTS

100% Labeling: Response of Multicellular Clusters and Cell Suspensions

Figure 1 illustrates the surviving fraction of cells maintained in multicellular clusters for 72 h as a function of ^{3}H activity (mBq) per labeled cell. Also shown is the survival curve obtained when cells were prepared identically except for maintenance as a single-cell suspension for 72 h at 10.5°C [see ref. (19) for experimental details]. The data were fitted by least squares to the relationship

$$\mathrm{SF}=(1-b)\mathrm{e}^{-A/A_1}+b\mathrm{e}^{-A/A_2}, \quad (1)$$

where SF is the surviving fraction, A is the activity per labeled cell, and b, A_1 and A_2 are the fitted parameters. The parameters A_1 and A_2 are analogous to D_0 values for the first and second components, respectively. With $b = 0$ for monoexponential response, the fitted values of A_1 for cluster and suspension are 0.80 ± 0.02 and 0.76 ± 0.04 mBq/cell, respectively. The response of the cells to incorporated [^{3}H]dThd is essentially the same whether the cells are arranged in the form of a cluster or are maintained as a single-cell suspension. Therefore, this suggests that the cells within the cluster do not receive any significant exposure to radiation from their neighbors (i.e. no cross-irradiation).

100% Labeling: Modification of Response by DMSO and Lindane

The surviving fractions of cells in multicellular clusters assembled and maintained in the presence or absence of 10% DMSO are also shown in Fig. 1. A least-squares fit of the data for each treatment condition to Eq. (1) with $b = 0$ gives A_1 values of 1.5 ± 0.08 and 0.80 ± 0.02 mBq/cell for 10% and 0% DMSO, respectively (Table 1). The dose modification factor (DMF), which indicates the degree of protection provided to the labeled cells by 10% DMSO, is expressed by the ratio of A_1 values in the presence and absence of DMSO as follows (19, 23):

$$\mathrm{DMF}([^3\mathrm{H}]\mathrm{dThd},\ 10\%\ \mathrm{DMSO})=\frac{A_1\ (\text{with DMSO})}{A_1\ (\text{without DMSO})}. \quad (2)$$

As shown in Table 1, a DMF value of 1.9 ± 0.12 is obtained, which indicates that 10% DMSO is able to protect V79 cells against lethal damage in clusters when all cells are labeled with [^{3}H]dThd. As reported earlier (13), 100 μ*M* lindane did not have any effect on the survival of cells from a multicellular cluster when all cells were labeled with [^{3}H]dThd. This suggests that the bystander effect does not significantly contribute to the killing of radiolabeled cells.

50% Labeling: Modification of Response by DMSO and/or Lindane

Figure 2A shows the cell surviving fraction as a function of the level of radioactivity per labeled cell for multicellular clusters in which 50% of the cells were labeled with [^{3}H]dThd. The clusters were maintained in the presence of (1) MEMA, (2) 10% DMSO in MEMA, (3) 100 μ*M* lindane in MEMA, or (4) 10% DMSO + 100 μ*M* lindane in MEMA. As shown in Fig. 2A, a two-component exponential survival curve emerges when the data from each experimental condition are fitted to Eq. (1). As expected, the transition from the first to second component occurs near 50% survival. Table 1 summarizes the fitted parameters for

the different treatment conditions. The fitted parameters for cases (1) and (3) are slightly different from those obtained previously (13) because the new values include results of additional experiments not reported earlier. In the absence of any treatment, as the activity per labeled cell increases, the surviving fraction drops sharply to about 50% and then continues to drop, albeit with a shallower slope. The first component of the two-component survival curve represents killing of the radiolabeled cells, whereas the second component represents killing of unlabeled bystander cells (13). Addition of 10% DMSO afforded significant protection against lethal damage to unlabeled bystander cells. In fact, the value of A_2 changes from 4.8 ± 1.1 to 11.1 ± 2.1 mBq/labeled cell (Table 1). If one considers this change a consequence of modification of the bystander effects imparted by the labeled cells to unlabeled cells, then the bystander modification factor (BMF) is defined as3

$$\mathrm{BMF}=\frac{A_2\ (\text{with treatment})}{A_2\ (\text{without treatment})}. \quad (3)$$

The bystander modification factor for 10% DMSO in multicellular clusters containing 50% cells labeled with [^{3}H]dThd is 2.3 ± 0.68 (Table 1). A greater degree of protection of the bystander cells was achieved with 100 μ*M* lindane (bystander modification factor = 3.8 ± 0.94). This value is within statistical uncertainties of the previously reported value of 3.5 ± 1.0 (13). The most dramatic protection of the bystander cells was manifested by a combined treatment of 10% DMSO and 100 μ*M* lindane, which yields a sharp drop in the response curve to about 50% survival and only limited cell killing at higher activities per labeled cell (Fig. 2A). Under this experimental condition, a bystander modification factor of 6.1 ± 1.5 was obtained.

10% Labeling: Modification of Response by DMSO and/or Lindane

The multicellular clusters were also prepared with a mixture of 10% radiolabeled cells and 90% unlabeled cells. As in the case for 50% labeling, Fig. 2B shows a similar two-component exponential response for each treatment condition. As expected, the transition from the first to second component for 10% labeling occurs near 90% survival. The parameters resulting from least-squares fits to Eq. (1) are given in Table 1. The bystander modification factors corresponding to 10% DMSO, 100 μ*M* lindane, and 10% DMSO + 100 μ*M* lindane are 1.4 ± 0.10, 1.8 ± 0.15, and 2.3 ± 0.17, respectively (Table 1). These values for the case of 10% labeling were of lesser magnitude than those for the 50% labeling. However, like the data for 50% labeling, the data for 10% labeling show that the killing of unlabeled bystander cells does not saturate even though the number of labeled cells that come in contact with unlabeled cells is five times less than in the case of the 50% labeling.

Biokinetics of [^{3}H]dThd in Cells

The uptake, maintenance and clearance of [^{3}H]dThd in V79 cells as they proceed through different stages of the experiment are depicted in Fig. 3. The area under the curve is proportional to the cumulated activity (decays) of ^{3}H in V79 cell nuclei. The period of 0–12 h represents the uptake of the radiochemical at 37°C. Previous studies have shown that the uptake is linear in time during this period (23). The period of 12–84 h represents the 72-h period in which the cells were maintained at 10.5°C in the cluster configuration. As expected, the cellular activity did not change during this period. Finally, the curved region corresponds to the 1-week period of colony formation at 37°C, where the cellular activity

[3]In our previous communication, we designated the ratio of the A_2 values as a bystander blocking factor. This name was selected because lindane is a gap junction inhibitor in V79 cells. The change in name to bystander modification factor acknowledges the fact that other agents such as DMSO can modify the response through other mechanisms.

has an effective half-time of ~12 h, which is in agreement with previous data (23). Integration under the curve and normalizing to 1 mBq give the mean cumulated activity (decays) in a labeled cell, $\tilde{A}$ = 343 Bq s per mBq in the cell. Finally, it should be noted that about 76% of the intracellular decays occurred while the cells were maintained in the cluster configuration at 10.5°C (23).

No Migration of Radioactivity in Multicellular Clusters

The multicellular clusters consisting of 50% radiolabeled and dyed cells and 50% unlabeled and undyed cells were maintained at 10.5°C for 72 h, dispersed, and analyzed by flow cytometry to verify percentage of cells dyed. The analysis of CFDA-positive and CFDA-negative cells is shown in Fig. 4A. The data confirm that 49.6% of the cells were dye-positive (M1 gate) and hence labeled with [^{3}H]dThd. The dye-negative cells (M2 gate) were then sorted and again analyzed by flow cytometry (Fig. 4B). Figure 4B shows that the undyed cells (M2 gate) were separated to a purity of ~97%. Aliquots of these cells were counted for radioactivity, and it was determined that they contained an average of 0.013 mBq/cell. The M1-gated (dye-positive) cells shown in Fig. 4A contained 1.5 mBq/cell. Since the dye-negative cells have a 3% contamination of radiolabeled and dyed cells, this population should have an average of at least 0.045 mBq/cell. This is well above the 0.013 mBq/cell observed. Therefore, these data provide strong evidence that there is no migration of [^{3}H]dThd from radiolabeled cells to surrounding unlabeled cells under the experimental conditions used.

Absorbed Dose to Labeled and Unlabeled Cells

The short-range β particles emitted by ^{3}H have a spectrum of energies from 0–18.6 keV (24), with ranges in water from 0–7 μm. The mean energy of the electron is only 5.7 keV, and it has a range of 1 μm in water. The mean diameter of a V79 cell is 10 μm, and the mean diameter of its nucleus is 8 μm (25). Using the model of Goddu *et al.* (26) and the full ^{3}H β-particle spectrum, the mean self-absorbed dose to the nucleus of a labeled cell per unit cumulated activity in the nucleus of the labeled cell is $S_{\text{self}}(\text{labeled}\leftarrow\text{labeled}) = 2.61 \times 10^{-3}$ Gy/Bq s. The mean self-absorbed dose to the nucleus, $D_{\text{self}}(\text{labeled})$, is $\tilde{A}$ $S_{\text{self}}(\text{labeled}\leftarrow\text{labeled}) = 0.895$ Gy per mBq in the cell. Therefore, the mean lethal dose for 100% labeling is D_{37} = 0.80 mBq (0.895 Gy/mBq) = 0.72 Gy. In contrast, the mean cross-dose to a neighboring unlabeled cell per unit cumulated activity in a single labeled cell is $S_{\text{cross}}(\text{unlabeled}\leftarrow\text{labeled}) = 3.03 \times 10^{-6}$ Gy/Bq s. For 50% labeling, each unlabeled cell has 12 neighbors, 6 of which are labeled (26). Therefore,

$S^{\text{total}}_{\text{cross}}(\text{unlabeled} \leftarrow \text{labeled}) = 1.82 \times 10^{-5}$ Gy/Bq s and $D^{\text{total}}_{\text{cross}}(\text{unlabeled} \leftarrow \text{labeled}) = 0.00624$ Gy mBq^{-1} in the labeled cell. Therefore, the dose to the labeled cell is over 140 times that to the unlabeled cell.

Functional GJIC in Multicellular Clusters

The fluorescent dye calcein AM was used to ascertain the presence of functional GJIC. As shown in Fig. 5A, the background fluorescence associated with undyed cells resulted in a single low-intensity peak with a geometric mean of 2.9. When 100% of the cells were dyed, a single broad and intense peak was observed with a geometric mean of 290 (Fig. 5B). When 50% of the cells were loaded with the dye, two peaks emerged with geometric means of 13 and 203, respectively (Fig. 5C). The peak corresponding to initially undyed cells has shifted markedly to the right, indicating that dye has been transferred from dyed to undyed cells. Hence functional GJIC is present in the V79 multicellular clusters maintained at 10.5°C. Addition of lindane inhibited dye transfer, as shown by the similarity of its histogram (Fig. 5D, geometric means of 9 and 225) to that of the 50% control culture, where

no dye transfer was possible (Fig. 5E, geometric means of 6 and 260). These data support the capacity of lindane to attenuate GJIC under the present experimental conditions.

DISCUSSION

The present study has used a three-dimensional tissue culture model (13) to quantify the lethal effect of nonuniform distributions of [^{3}H]dThd. This model affords a high degree of control over the percentage of radiolabeled cells in the cluster. The short range of the ^{3}H β particles prevents significant irradiation of unlabeled cells by radioactivity in the labeled cells (13). This is supported by the data in Fig. 1 that show that the mean lethal ^{3}H activity per cell required to achieve 37% survival is essentially the same for 100% labeling regardless of whether the cells are maintained as clusters (0.80 ± 0.02 mBq/cell) or in suspension, where no cross-dose is possible (0.76 ± 0.04 mBq/cell). It is also supported by theoretical calculations for 50% labeling (see Results section) that yield mean absorbed doses to the labeled and unlabeled cells of 0.895 and 0.00624 Gy mBq^{-1} per labeled cell, respectively. Since the activity per labeled cell required to effect 1% survival is about 20 mBq per labeled cell (Fig. 2A), the dose to the unlabeled cells in this case would be about 0.12 Gy. Assuming an equal effectiveness per gray between self- and cross-irradiation (worst-case scenario), this would produce an SF of 0.84 in the unlabeled cells which comprise 50% of the population. If all of the labeled cells were killed, and the killing of unlabeled cells was due to irradiation of their nuclei, this would yield an expected SF for the entire population of about 0.42. Similar results emerge for the case of 10% labeling. The difference between 0.42 and the observed SF of 0.01 suggests that mechanisms other than cross-irradiation play the principal role in the observed killing of unlabeled bystander cells.

Three different radiolabeling conditions were investigated in which 100, 50 or 10% of the cells within the multicellular clusters were labeled, each resulting in markedly different survival curves. The data for 100% labeling in Fig. 1 yielded an exponential survival curve with a mean lethal cellular activity of 0.80 mBq/cell. In contrast, the data for 50 and 10% labeling required fits to a two-component exponential function (Fig. 2A, B). These fits and the resulting parameters (Table 1) indicate that about 50 and 10% of the cells are killed at relatively low activities per labeled cell because only the labeled cells are killed. However, the second components (Fig. 2) indicate that unlabeled cells are killed even though they do not receive significant irradiation. This strongly suggests that bystander effects are responsible for killing of unlabeled cells. Furthermore, the linearity of the second components suggests that the bystander signal increases exponentially with the dose to the labeled (irradiated) cells. This finding appears to differ from the data of Wu *et al.* (27), who found a saturation in the dose response for mutation induction in A_L cells irradiated through the cytoplasm with an α-particle microbeam. They observed a similar saturation in response when cell survival was used as the end point (data available only down to about 70% survival). They postulated that the saturation after eight α-particle traversals may have been due to the fact that the traversals were split between only two areas in the cytoplasm (27), suggesting that a more uniform irradiation of the cytoplasm may have eliminated the saturation. While this may be the case, the present data do not involve irradiation of the cytoplasm of the same cell; rather they involve death of unlabeled bystander cells adjacent to cells whose nucleus is irradiated by β particles emitted by [^{3}H]dThd. Therefore, given the very different irradiation conditions (cytoplasm of the same cell compared to the nucleus of a neighboring cell), it is possible that different mechanisms are operational, which could lead to different dose–response relationships. Furthermore, considering other differences between the experimental protocols (e.g. radiation type, cell type, dose of radiation to target cells, temperature, cell geometry), it is not surprising that differences were observed.

A more recent report from the same laboratory examined the mutagenic response in the surviving bystander cell population after irradiation of 0, 5, 10 or 20% of the cell nuclei with 20 α particles from the microbeam (28). Under these irradiation conditions, which were somewhat similar to those in the present study, they found a linear increase in the mutant fraction of bystander cells as the percentage of cell nuclei in the population that were hit with the 20 α particles was increased. A plateau was reached when 10% of the nuclei were hit such that there was no significant difference in mutation fraction when 20% of the cells in the population were hit. As indicated by the authors, this was perhaps expected in their two-dimensional monolayer model because the number of unirradiated cells in direct contact with an irradiated cell is not much different in the two cases. The data in the present work also suggest that percentage of cells labeled is an important determinant for bystander effects. However, in the present work, higher percentages of labeling appear to impart bystander effects more efficiently in the three-dimensional cluster model. The fitted values for A_2 (Table 1) differ by about 10-fold for 10% and 50% labeling, despite only a 5-fold difference in the percentage of cells labeled. Therefore, the efficiency of the transfer of bystander effects is reduced by a factor of two for 10% labeling compared to 50% labeling. It is possible that coupling of an average of about 1.2 radioactive cells to each bystander cell (10% labeling) results in transmission of damage signals to a single region of the bystander cell compared to a more uniform transmission when 6 radioactive cells are coupled to each bystander cell (50% labeling). This could lead to less efficient killing of the coupled bystander cell. Although we are not aware of any experimental data to support this hypothesis, this argument is analogous to that of Wu *et al.* (27) for cytoplasmic irradiation.

Gap junctional intercellular communication has been implicated as an important mediator of radiation-induced bystander effects (6). Gap junctions are intercellular membrane channels that directly link the interiors of neighboring cells. These channels have diameters of 1.5–2 nm and permit the direct passage of small (<2,000 Da) molecules between the cytoplasm of neighboring cells (29). V79 cells were reported to have some GJIC at physiological temperature (16–18, 30). It has also been shown by scrape-loading and dye transfer that V79 cells retained GJIC even when maintained for 72 h at 10.5°C as a confluent monolayer (13). While this served as evidence of GJIC in monolayers at 10.5°C, it was necessary to demonstrate the presence of functional coupling of V79 cells in multicellular clusters maintained at 10.5°C. This was studied in the present work by monitoring the transfer of the fluorescent dye calcein AM, which can traverse gap junctions, by flow cytometry. Figure 5 shows that functional gap junctions are indeed formed between the neighboring cells within the cluster, as shown by the transfer of calcein AM from dyed to undyed cells. Moreover, the current study also shows that GJIC between V79 cells in the multicellular cluster can be inhibited to some degree by lindane. This is in agreement with earlier findings (17, 31). It is perhaps not surprising that functional coupling occurs at 10.5°C. Ward *et al.* (32) have shown that V79 cells are able to repair DNA single-strand breaks at 10°C, albeit at a reduced rate. Double-strand breaks were not repaired at this temperature. Therefore, while 10.5°C does not represent normal body temperature, many important physiological processes such as repair and GJIC remain operational.

To elucidate the potential mechanisms responsible for bystander effects observed with 50 and 10% labeling, DMSO and/or lindane was added to the culture medium before the multicellular clusters were formed. Our results show that 10% DMSO offered a fair degree of protection of bystander cells in both labeling situations (Table 1). A better protective effect was afforded by 100 μ*M* lindane. However, concurrent treatment with DMSO and lindane brought about maximum protection of the bystander cells. For 50% labeling, the effect of a combined treatment was more prominent than for 10%, with bystander modification factor values of 6.1 ± 1.5 and 2.3 ± 0.17, respectively. This difference may be explained in light of the interactions between the labeled and unlabeled cells. The metabolic

generation of ROS due to oxidative stress after exposure to ionizing radiation has recently been hypothesized as a mediator of bystander responses in unirradiated cells (10, 33). Exposure to high concentrations of ROS results in a wide spectrum of DNA damage, cell cycle arrest, senescence, and eventually cell death (1, 34–36). In the present study, significant protection (DMF = 1.9 ± 0.12) was afforded by DMSO against killing of cells in multicellular clusters in which 100% of the cells were labeled. The intracellular generation of of $^{\bullet}$OH by ^{3}H decays may be the principal cause of cell death. DMSO is a potent scavenger of $^{\bullet}$OH (37), and it is therefore expected to attenuate the effect of [^{3}H]dThd provided that an adequate concentration of DMSO is used (19). However, $^{\bullet}$OH are short-lived and can diffuse only about 4 nm (38). Thus, while these $^{\bullet}$OH may account for lethal damage to labeled cells in the case of 100% labeling, no transmissible lethality to unlabeled bystander cells should occur with this source of $^{\bullet}$OH. However, it is possible that there could be more persistent production of $^{\bullet}$OH from another source such as superoxide ($O_2^{\bullet -}$) (10, 39). It is possible that free radicals, particularly $^{\bullet}$OH, produced through these mechanisms could lead to membrane lipid peroxidation and consequent formation of a number of free radicals capable of producing DNA damage and cell death (40–42). While DMSO could block some of the above events in labeled cells and thereby reduce the concentration of free radicals in bystander cells, it is possible that some of the long-lived radicals that are not scavenged by DMSO may escape through gap junctions, reach the neighboring cells, and subsequently inflict lethal damage on these cells. The ability of lindane to block gap junctions may prevent the radicals from reacting with the DNA of bystander cells. However, lindane may not entirely abolish GJIC and provide complete protection against damage to the bystander cells by ROS originating in the labeled cells. This is likely in view of the fact that lindane affects GJIC by altering the permeability of gap junction channels and the number of gap junctions (16, 43). Further support for this is provided by the data in Fig. 5D, which shows that GJIC-mediated dye transfer was not completely blocked by lindane. Based on the above arguments, the presence of both DMSO and lindane might be expected to have an impact on both the $^{\bullet}$OH-initiated events in the labeled cells and their propagation through gap junctions to the bystander cells. This may explain why the bystander modification factor is greater for the combined treatment with DMSO and lindane compared to treatment with either agent alone (Table 1).

Our results with lindane indicating the involvement of GJIC in bystander effects caused by nonuniform distributions of incorporated radioactivity are consistent with those of Azzam *et al.* (6), who reported a similar reduction of α-particle-induced bystander effects in human diploid fibroblast cell population by lindane. Recently, Zhou *et al.* (28) have provided evidence that irradiation of human–hamster A_L cells induces a bystander mutagenic response in unir-radiated neighboring cells that can be inhibited by lindane but not by DMSO. They concluded that a signal transduction pathway other than $^{\bullet}$OH-mediated oxidative stress might play a role in mediating the bystander responses for α particles. Although the present study with β particles implicates $^{\bullet}$OH as the primary oxidant species responsible for the initiation of damage to bystander cells, it is also possible that other signaling mechanisms triggered by ROS may be involved as proposed by Iyer and Lehnert (12). In this context, it should be mentioned that oxidative stress has been correlated with the induction of signal transduction that is linked to a variety of deleterious effects of radiation (34, 44–46).

In conclusion, the present study provides new data on the biological effects of nonuniform distributions of incorporated radioactivity using a novel approach to specifically control the degree of nonuniformity. This study also establishes the response of V79 multicellular clusters to incorporated radioactivity and furnishes substantial evidence that bystander effects play a significant role in determining the biological effect of incorporated radioactivity. Furthermore, these data suggest that at least a part of the observed bystander

effects are initiated by free radicals and mediated through gap junctions. These findings may ultimately enhance our capacity to predict the biological response of tumor and normal tissue in nuclear medicine and from environmental exposure to radioactivity.

Acknowledgments

The authors greatly appreciate the insightful comments and suggestions provided by Drs. Edouard I. Azzam and Sonia M. de Toledo, Department of Radiology, UMDNJ–New Jersey Medical School. We are also thankful to Thomas N. Denny for providing access to the FACS. This work was supported in part by USPHS Grant Nos. R01 CA83838 (RWH) and shared instrumentation grant 1 S10 RR14753-01 (TND).

REFERENCES

1. Iyer R, Lehnert BE. Effects of ionizing radiation in targeted and nontargeted cells. Arch. Biochem. Biophys. 2000; 376:14–25. [PubMed: 10729186]
2. Nagasawa H, Little JB. Induction of sister chromatid exchanges by extremely low doses of alpha-particles. Cancer Res. 1992; 52:6394–6396. [PubMed: 1423287]
3. Nagasawa H, Little JB. Unexpected sensitivity to the induction of mutations by very low doses of alpha-particle irradiation: Evidence for a bystander effect. Radiat. Res. 1999; 152:552–557. [PubMed: 10521933]
4. Deshpande A, Goodwin EH, Bailey SM, Marrone BL, Lehnert BE. Alpha-particle-induced sister chromatid exchange in normal human lung fibroblasts: Evidence for an extranuclear target. Radiat. Res. 1996; 145:260–267. [PubMed: 8927692]
5. Hickman AW, Jaramillo RJ, Lechner JF, Johnson NF. Alpha-particle-induced p53 protein expression in a rat lung epithelial cell strain. Cancer Res. 1994; 54:5797–5800. [PubMed: 7954402]
6. Azzam EI, de Toledo SM, Gooding T, Little JB. Intercellular communication is involved in the bystander regulation of gene expression in human cells exposed to very low fluences of alpha particles. Radiat. Res. 1998; 150:497–504. [PubMed: 9806590]
7. Prise KM, Belyakov OV, Folkard M, Michael BD. Studies on bystander effects in human fibroblasts using a charged particle microbeam. Int. J. Radiat. Biol. 1998; 74:793–798. [PubMed: 9881726]
8. Mothersill C, Seymour C. Medium from irradiated human epithelial cells but not human fibroblasts reduces the clonogenic survival of unirradiated cells. Int. J. Radiat. Biol. 1997; 71:421–427. [PubMed: 9154145]
9. Lehnert BE, Goodwin EH. Extracellular factor(s) following exposure to alpha particles can cause sister chromatid exchanges in normal human cells. Cancer Res. 1997; 57:2164–2171. [PubMed: 9187116]
10. Narayanan PK, Goodwin EH, Lehnert BE. Alpha particles initiate biological production of superoxide anions and hydrogen peroxide in human cells. Cancer Res. 1997; 57:3963–3971. [PubMed: 9307280]
11. Narayanan PK, LaRue KEA, Goodwin EH, Lehnert BE. Alpha particles induce the production of interleukin-8 by human cells. Radiat. Res. 1999; 152:57–63. [PubMed: 10381841]
12. Iyer R, Lehnert BE. Factors underlying the cell growth-related bystander responses to alpha particles. Cancer Res. 2000; 60:1290–1298. [PubMed: 10728689]
13. Bishayee A, Rao DV, Howell RW. Evidence for pronounced bystander effects caused by nonuniform distributions of radioactivity using a novel three-dimensional tissue culture model. Radiat. Res. 1999; 152:88–97. [PubMed: 10428683]
14. Mothersill C, Seymour CB. Cell–cell contact during gamma irradiation is not required to induce a bystander effect in normal kidney keratinocytes: Evidence for release during irradiation of a signal controlling survival into the medium. Radiat. Res. 1998; 149:252–262.
15. Kroemer G. The proto-oncogene Bcl-2 and its role in regulating apoptosis. Nat. Med. 1997; 3:614–620. [PubMed: 9176486]
16. Yancey SB, Edens JE, Trosko JE, Chang CC, Revel JP. Decreased incidence of gap junctions between Chinese hamster V-79 cells upon exposure to the tumor promoter 12-*o*-tetradecanoyl phorbol-13-acetate. Exp. Cell Res. 1982; 139:329–340. [PubMed: 7084321]

17. El-Fouly MH, Trosko JE, Chang CC. Scrape-loading and dye transfer: A rapid and simple technique to study gap junctional intercellular communication. Exp. Cell. Res. 1987; 168:422–430. [PubMed: 2433137]
18. Banrud H, Mikalsen SO, Berg K, Moan J. Effects of ultraviolet radiation on intercellular communication in V79 Chinese hamster fibroblasts. Carcinogenesis. 1994; 15:233–239. [PubMed: 8313514]
19. Bishayee A, Rao DV, Bouchet LG, Bolch WE, Howell RW. Radioprotection by DMSO against cell death caused by intracellularly localized iodine-125, iodine-131 and polonium-210. Radiat. Res. 2000; 153:416–427. [PubMed: 10761002]
20. Goldberg GS, Beckberger JF, Naus CCG. A pre-loading method of evaluating gap junctional communication by fluorescent dye transfer. BioTechniques. 1995; 18:490–497. [PubMed: 7779401]
21. Zhang W, Couldwell WT, Simard MF, Song H, Lin JHC, Nedergaard M. Direct gap junction communication between malignant glioma cells and astrocytes. Cancer Res. 1999; 59:1994–2003. [PubMed: 10213512]
22. Tomasetto C, Nepeu MJ, Daley J, Horan PK, Sager R. Specificity of gap junction communication among human mammary cells and connexin transfectants in culture. J. Cell Biol. 1993; 122:157–167. [PubMed: 8391000]
23. Howell RW, Goddu SM, Bishayee A, Rao DV. Radioprotection against lethal damage caused by chronic irradiation with radionuclides *in vitro*. Radiat. Res. 1998; 150:391–399. [PubMed: 9768852]
24. Browne, E.; Firestone, RB. Table of Radioactive Isotopes. New York: Wiley; 1986.
25. Howell RW, Rao DV, Hou D-Y, Narra VR, Sastry KSR. The question of relative biological effectiveness and quality factor for Auger emitters incorporated into proliferating mammalian cells. Radiat. Res. 1991; 128:282–292. [PubMed: 1961925]
26. Goddu SM, Rao DV, Howell RW. Multicellular dosimetry for micrometastases: Dependence of self-dose versus cross-dose to cell nuclei on type and energy of radiation and subcellular distribution of radionuclides. J. Nucl. Med. 1994; 35:521–530. [PubMed: 8113908]
27. Wu LJ, Randers-Pehrson GR, Xu A, Waldren CA, Geard CR, Yu ZL, Hei TK. Targeted cytoplasmic irradiation with alpha particles induces mutations in mammalian cells. Proc. Natl. Acad. Sci. USA. 1999; 96:4959–4964. [PubMed: 10220401]
28. Zhou H, Randers-Pehrson G, Waldren CA, Vannais D, Hall EJ, Hei TK. Induction of a bystander mutagenic effect of alpha particles in mammalian cells. Proc. Natl. Acad. Sci. USA. 2000; 97:2099–2104. [PubMed: 10681418]
29. Trosko JE, Ruch RJ. Cell–cell communication in carcinogenesis. Front. Biosci. 1998; 3:208–236.
30. Zeilmaker MJ, Yamasaki H. Inhibition of junctional intercellular communication as a possible short-term test to detect tumor-promoting agents: Results with nine chemicals tested by dye transfer assay in Chinese hamster V79 cells. Cancer Res. 1986; 46:6180–6186. [PubMed: 3779639]
31. Tsushimoto G, Chang CC, Trosko JE, Matsumura F. Cytotoxicity, mutagenic, and cell–cell communication inhibitory properties of DDT, lindane, and chlordane on hamster cells *in vitro*. Arch. Environ. Contam. Toxicol. 1983; 12:721–730. [PubMed: 6197034]
32. Ward JF, Limoli CL, Calabro-Jones PM, Aguilera J. An examination of the repair saturation hypothesis for describing shouldered survival curves. Radiat. Res. 1991; 127:90–96. [PubMed: 2068276]
33. Clutton SM, Townsend KMS, Walker C, Ansell JD, Wright EG. Radiation-induced genomic instability and persisting oxidative stress in primary bone marrow cultures. Carcinogenesis. 1996; 17:1633–1639. [PubMed: 8761419]
34. Chen Q, Ames BN. Senescence-like growth arrest induced by hydrogen peroxide in human diploid fibroblast F65 cells. Proc. Natl. Acad. Sci. USA. 1994; 91:4130–4134. [PubMed: 8183882]
35. McLennan G, Oberley LW, Autor A. The role of oxygen-derived free radicals in radiation-induced damage and death of non-dividing eukaryotic cells. Radiat. Res. 1980; 84:122–132. [PubMed: 7454975]

36. Spencer JE, Jenner A, Aruoma OI, Cross CE, Wu R, Halliwell B. Oxidative DNA damage in human respiratory tract epithelial cells. Time course in relation to DNA strand breakage. Biochem. Biophys. Res. Commun. 1996; 224:17–22. [PubMed: 8694807]

37. Raju MR, Schillachi ME, Carpenter SG, Goodhead DT, Ward JF. Radiobiology of ultrasoft X rays. V. Modification of cell inactivation by dimethyl sulfoxide. Radiat. Res. 1996; 145:563–567. [PubMed: 8619021]

38. Roots R, Okada S. Protection of DNA molecules of cultured mammalian cells from radiation-induced single-strand scissions by various alcohols and SH compounds. Int. J. Radiat. Biol. 1972; 21:329–342.

39. Riley PA. Free radicals in biology: Oxidative stress and the effects of ionizing radiation. Int. J. Radiat. Biol. 1994; 65:27–33. [PubMed: 7905906]

40. Peter B, Wartena M, Kampinga HH, Konings AWT. Role of lipid peroxidation and DNA damage in paraquat toxicity and the interaction of paraquat with ionizing radiation. Biochem. Pharmacol. 1992; 43:705–715. [PubMed: 1540224]

41. Limoli CL, Hartmann A, Shephard L, Yang C, Boothman DA, Bartholomew J, Morgan WF. Apoptosis, reproductive failure, and oxidative stress in Chinese hamster ovary cells with compromised genomic integrity. Cancer Res. 1998; 58:3712–3718. [PubMed: 9721883]

42. Higuchi Y, Matsukawa S. Glutathione depletion induces giant DNA and high-molecular-weight DNA fragmentation associated with apoptosis through lipid peroxidation and protein kinase C activation in C6 glioma cells. Arch. Biochem. Biophys. 1999; 363:33–42. [PubMed: 10049497]

43. Guan X, Bonney WJ, Ruch RJ. Changes in gap junction permeability, gap junction number, and connexin43 expression in lindane- treated rat liver epithelial cells. Toxicol. Appl. Pharmacol. 1995; 130:79–86. [PubMed: 7530866]

44. Trosko JE, Inoue T. Oxidative stress, signal transduction, and intercellular communication in radiation carcinogenesis. Stem Cells. 1997; 15(Suppl. 2):59–67. [PubMed: 9368287]

45. Burdon RH. Superoxide and hydrogen peroxide in relation to mammalian cell proliferation. Free Radic. Biol. Med. 1995; 18:775–795. [PubMed: 7750801]

46. Remacle J, Raes M, Toussaint O, Renard P, Rao G. Low levels of reactive oxygen species as modulators of cell function. Mutat. Res. 1995; 316:103–122. [PubMed: 7862174]

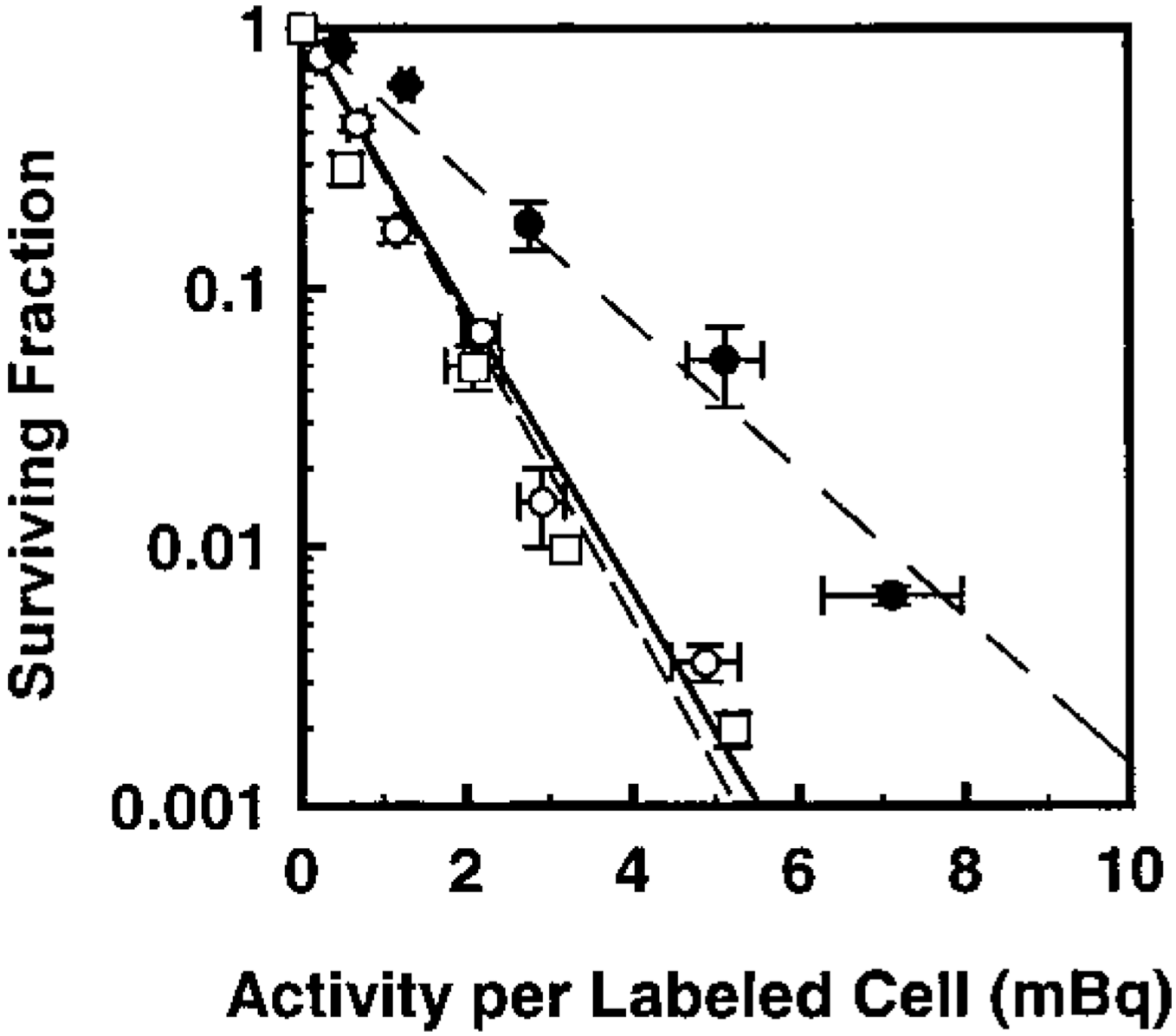

FIG. 1.

Survival of V79 cells as a function of activity per labeled cell wherein 100% of the cell population was labeled with [^{3}H]dThd. Cells were maintained in MEMA as multicellular clusters in the absence (○) and presence (●) of 10% DMSO, or as suspensions in the absence of DMSO (□). Data points represent the average of eight (○), three (●) and two (□) experiments, respectively. Standard errors are shown accordingly.

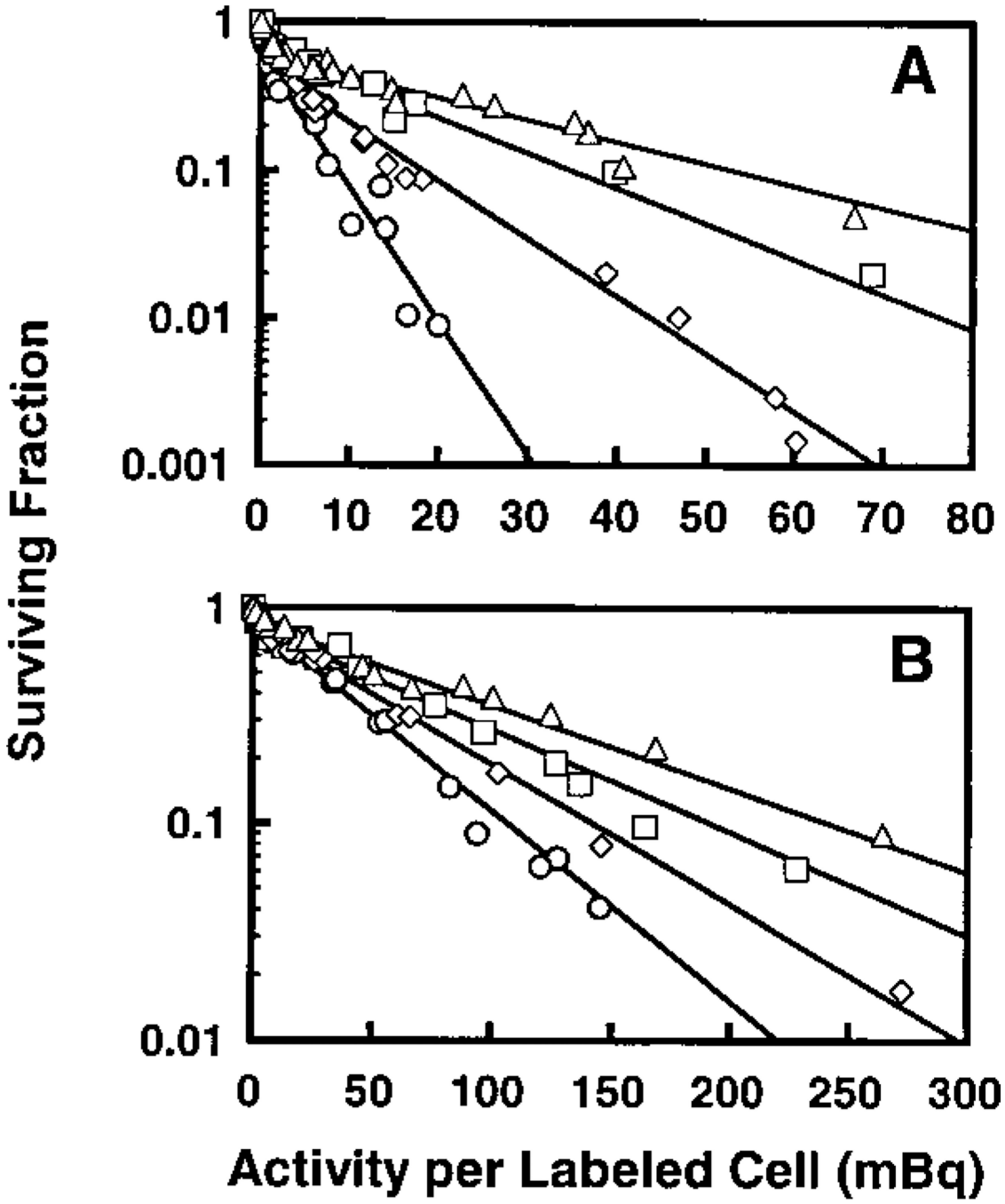

FIG. 2.

Survival of V79 cells as a function of activity per labeled cell in which 50% (panel A) or 10% (panel B) of the cells were labeled with [^{3}H]dThd and used to form multicellular clusters. The clusters were maintained in MEMA (○), 10% DMSO in MEMA (◊), 100 μ*M* lindane in MEMA (□), or 10% DMSO + 100 μ*M* lindane in MEMA (△). Data from two to five independent experiments are presented for each treatment. Standard errors for each data point are of the order of the dimensions of the symbols.

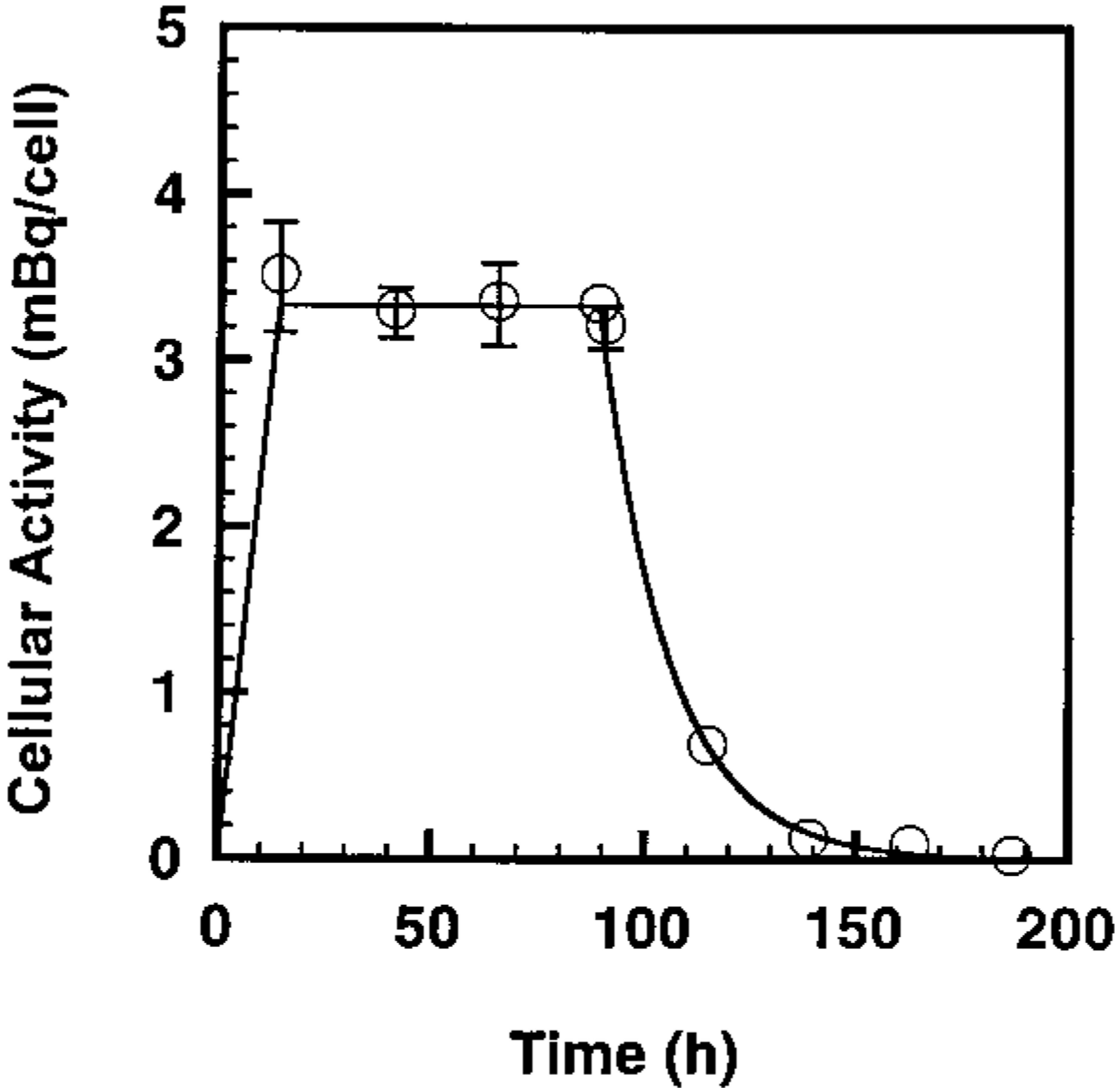

FIG. 3.

Intracellular ^{3}H activity in V79 cells as a function of time. The period 0–12 h represents the uptake of the radiochemical. The period 12–84 h represents the 72-h period in which the cells were maintained at 10.5°C. The period beyond 84 h corresponds to the 1-week period of colony formation, when the cellular activity has an effective half-time of ~12 h. The area under the curve is proportional to the cumulative decays in the V79 cell nucleus. Approximately 76% of the intracellular decays occur when the cells were maintained at 10.5°C.

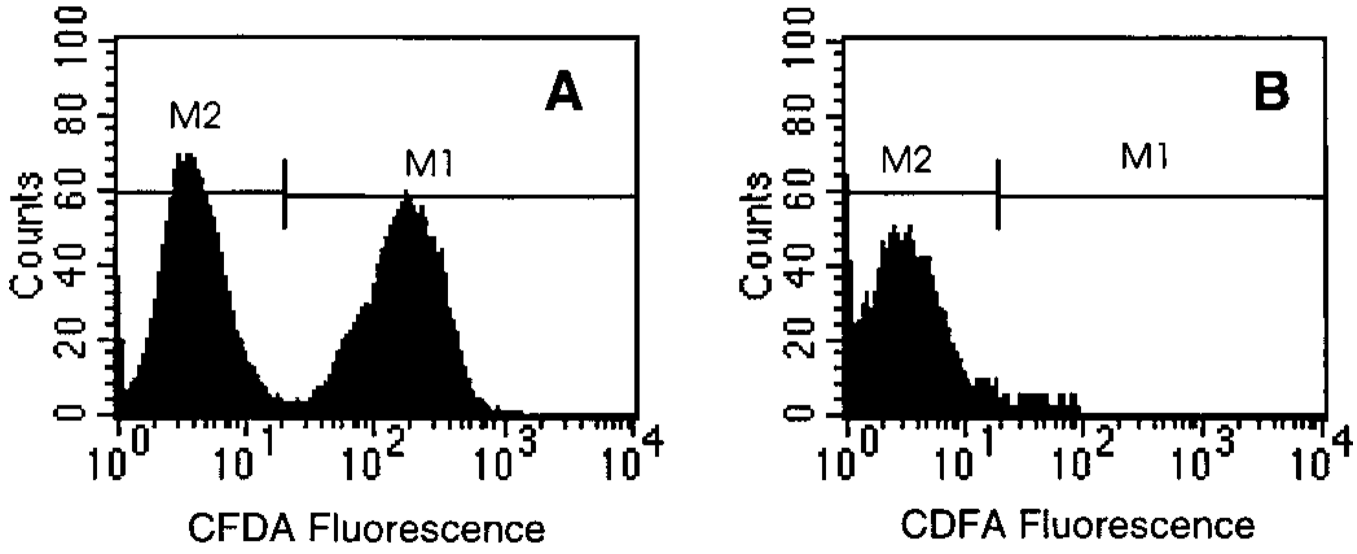

FIG. 4.

Evidence of no migration of radioactivity from labeled to unlabeled cells in multicellular cluster containing 50% labeled cells. V79 cells were radiolabeled with [^{3}H]dThd, dyed with CFDA, and mixed with unlabeled and undyed cells, and cell clusters were prepared and maintained at 10.5°C for 72 h. Panel A: After 72 h, flow cytometry analysis shows that 49.6% of the cells remained dyed (M1). Panel B: The undyed cells (M2) were separated from the dyed cells (M1) by FACS. No significant radioactivity was found in the undyed cells.

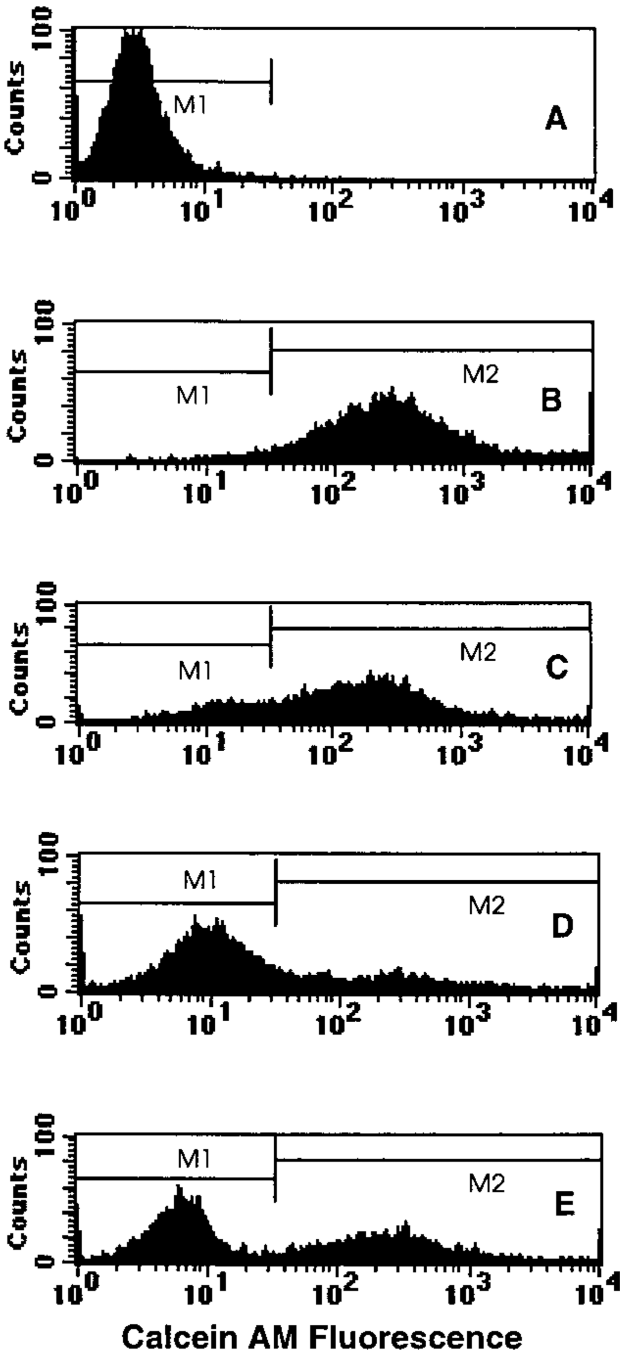

FIG. 5.

Single-parameter histogram from flow cytometry of V79 cells from a multicellular cluster containing (panel A) 0%, (panel B) 100% or (panel C) 50% dyed cells, (panel D) 50% dyed cells in the presence of 100 μ*M* lindane, or (panel E) an equal mixture of 0% and 100% dyed cells followed by immediate analysis. Transfer of the fluorescent dye calcein AM from dyed to undyed cells in the case of 50% dyed cells is seen in the right lateral shift in the peak position corresponding to the cells that were initially undyed (panel C). Addition of lindane dramatically reduces the degree of dye transfer (panel D) as seen in the similarity to the 50% control histogram, where no dye transfer was possible (panel E).

TABLE 1

Fitted Parameters for Survival Curves and Bystander Modification Factor for Multicellular Clusters

Treatment	Percentage of cells labeled	Number of experiments	*b*	A_1[a] (mBq/labeled cell)	A_2[a] (mBq/labeled cell)	Bystander modification factor[b]
[^{3}H]dThd	100	8	0	0.80 ± 0.02[c]	—	—
[^{3}H]dThd + 10% DMSO	100	2	0	1.5 ± 0.08	—	1.9 ± 0.12[d]
[^{3}H]dThd	50	4	0.61 ± 0.09	0.29 ± 0.16	4.8 ± 1.1	—
[^{3}H]dThd + 10% DMSO	50	5	0.52 ± 0.08	1.5 ± 0.28	11.1 ± 2.1	2.3 ± 0.68
[^{3}H]dThd + 100 μ*M* lindane	50	3	0.68 ± 0.03	0.72 ± 0.15	18.2 ± 2.0	3.8 ± 0.94
[^{3}H]dThd + 10% DMSO + 100 μ*M* lindane	50	3	0.61 ± 0.03	1.1 ± 0.20	29.5 ± 2.8	6.1 ± 1.5
[^{3}H]dThd	10	2	0.87 ± 0.02	0.96 ± 0.40	49.4 ± 1.9	—
[^{3}H]dThd + 10% DMSO	10	2	0.84 ± 0.02	1.4 ± 0.65	67.0 ± 4.3	1.4 ± 0.10
[^{3}H]dThd + 100 μ*M* lindane	10	2	0.82 ± 0.02	1.4 ± 0.77	91.0 ± 6.7	1.8 ± 0.15
[^{3}H]dThd + 10% DMSO + 100 μ*M* lindane	10	2	0.86 ± 0.03	3.5 ± 1.8	112.4 ± 7.5	2.3 ± 0.17

[a] A_1 and A_2 are analogous to the D_0's of the first (labeled cells) and second (bystander cells) components of the fitted survival curve (Eq. 1).

[b] A_2 (with treatment)/A_2 (without treatment).

[c] Mean ± SE.

[d] For 100% labeling, this quantity represents the traditional dose modification factor (DMF).